Aalborg Universitet

AALBORG UNIVERSITY
DENMARK

Wide-Band and Wide-Angle Scanning Phased Array Antenna for Mobile Communication System

Yang, Guangwei; Zhang, Yiming; Zhang, Shuai

Published in:
IEEE Open Journal of Antennas and Propagation

DOI (link to publication from Publisher):
10.1109/OJAP.2021.3057062

Creative Commons License
Unspecified

Publication date:
2021

Document Version
Accepted author manuscript, peer reviewed version

Link to publication from Aalborg University

Citation for published version (APA):
Yang, G., Zhang, Y., & Zhang, S. (2021). Wide-Band and Wide-Angle Scanning Phased Array Antenna for Mobile Communication System. *IEEE Open Journal of Antennas and Propagation*, *2*, 203-212. Article 9347484. Advance online publication. https://doi.org/10.1109/OJAP.2021.3057062

General rights
Copyright and moral rights for the publications made accessible in the public portal are retained by the authors and/or other copyright owners and it is a condition of accessing publications that users recognise and abide by the legal requirements associated with these rights.

- Users may download and print one copy of any publication from the public portal for the purpose of private study or research.
- You may not further distribute the material or use it for any profit-making activity or commercial gain
- You may freely distribute the URL identifying the publication in the public portal -

Take down policy
If you believe that this document breaches copyright please contact us at vbn@aub.aau.dk providing details, and we will remove access to the work immediately and investigate your claim.

Wide-band and Wide-Angle Scanning Phased Array Antenna for Mobile Communication System

Guangwei Yang, *Member, IEEE,* Yiming Zhang, *Member, IEEE,*
and *Shuai Zhang,* Senior *Member, IEEE*

***Abstract*—A wide-band phased array antenna with wide-angle scanning capability for mobile communication system is proposed in this paper. An air cavity is properly embedded into the substrate under each array element. This method is very simple and can efficiently enhance wide-angle scanning performance by improving the wide-angle scanning impedance matching (WAIM) and realizing the beam-width of elements in the array. Besides, the operating bandwidth is also extended with the proposed approach. The wide-angle scanning capability is analyzed and verified by both the linear array antennas (on large ground planes in detail) and the planar array. Two 1×8 linear arrays and one 8×8 planar array are demonstrated, which achieve the beam scanning of around ±60° with a realized gain reduction under 3.5 dB in the wide operating bandwidth (37.4%). Furthermore, the beam in the E-plane can scan over ±70° with a realized gain reduction under less than 3 dB. Two linear array prototypes with wide-angle scanning capacity in two planes are fabricated and characterized, yielding good performance within overall operational bandwidth. The measured results align very well with the simulated. The proposed wideband phased array with large scanning coverage is a promising candidate for 5G mobile communications.**

***Index Terms*—mobile communication, phased arrays, vehicle antennas, beamforming, scanning antennas.**

I. Introduction

With the rapid development of electronic technology, phased array antennas have been applied not only in the defense and military fields, but also in civil fields, such as radar, satellite communications, astronomy and meteorology, air traffic, earth detection, space exploration, remote sensing mapping, driverless, and biomedicine, especially 5G communications [1-2]. The multi-domain requirements of phased array antennas have led to increasingly higher performance requirements for phased array antennas, such as multifunction, low cost, and fast and flexible changes in beams, especially wider beam scanning coverage. Therefore, the issue of wide-angle scanning of phased array antennas has become a hotspot and main topic for global researchers and scholars.

There are many methods have been applied to achieve more excellent phased array antennas with large-angle scanning capability [3]-[18]. Firstly, extending the element pattern of the array is a useful method to improve the scanning coverage of phased arrays [3]-[8]. The methods such as the metal-cavity [3], special structures and metal via [4], using metal walls [5], designing the tapered slot [6], and proposing a resonant microstrip meander line [7] are applied to extend the radiation element pattern. Secondly, pattern-reconfigurable technology is an effective measure for phased arrays with large scanning coverage improvement [9]-[11]. Thirdly, the mutual coupling among the elements in the array plays a pivotal role to achieve large-angle scanning capability in linear or planar arrays [12]-[15]. Mutual coupling among array elements varies with array scanning angles, which changes the impedance of each array element at different scan angles. Some techniques are applied to enhance the WAIM of array antennas such as: adding the dielectric sheet above the arrays [12], using a multilayer dielectric as the ground plane [13], loading a dielectric layer with metal patches upon waveguides [14], and implementing split-ring resonators (SRRs) in front of the dipole array [15]. Besides, some combined techniques are introduced to enlarge the scanning coverage of phased array antennas, such as combining mechanical and electrical scanning technology [16], multi-plane array technology [17], hemispherical lens technology [18], and so on. For tightly coupled techniques [19] [20] are also applied to achieve the wide-angle scanning capability in a wide band. However, the tightly coupling technology is not suitable for 5G communication systems, because the coupling of the element in the array is very strong. Although the decoupling network [21] is applied to improve its coupling characteristics, it is difficult to satisfy the requirement of the 5G communication system. Besides, some other methods have been presented to provide some useful research direction, although, the scanning capability has some limitation. Graded-index meta-surface (GIMS) lens are applied to instead the shift phaser to realize beam scanning capability [22]. The phase gradient meta-surface is designed to extend the scanning coverage [23]. A 1-bit reconfigurable reflectarray technology is presented to realize wide-angle scanning capability in [24]. Although, the above methods can realize scanning ability of the phased array, some other issues such as complex structure, scanning accuracy of the beam, efficiency, gain fluctuation should be solved.

In this work, a novel and efficient approach will be introduced to enhance the beam scanning coverage with low gain reduction and the impedance bandwidth of a phased array antenna, where a mixed dielectric substrate with an air-cavity structure is applied. The proposed array is suitable for the mobile communication

Manuscript received December 23, 2020; revised January 15, 2021. This work has been supported by AAU Young Talent Program. (Corresponding author: *Shuai Zhang*)

The authors are with are with the Antennas, Propagation and Millimeter-Wave Systems Section, Department of Electronic Systems, Aalborg University, 9220 Aalborg, Denmark. (E-mail gwyang086@es.aau.dk; sz@es,aau.dk; yiming@es.aau.dk).

Guangwei Yang is also with the School of Electronic Engineering and Computer Science, Queen Mary University of London, London E1 4NS, UK.

system because of low profile. The novelties in this paper are mainly presented:

(a) A new approach is presented to improve WAIM, which is different from the above references, and adjust the height of the air-cavity in the substrate to realize WAIM.

(b) The proposed approach can not only improve WAIM, but also realize the broad the element beam-width in the array. And the 3-dB beam-width is up to more than 140° in the E-plane and 120° in the H-plane in the array, respectively.

(c) Besides, the bandwidth of the antenna can be broadened as well by the proposed approach.

(d) The low-profile phased array with large scanning coverage is designed and applied in the mobile communication system.

This work is mainly introduced from the following aspects: the antenna design and the performance of the phased array will be introduced and studied in Section II. The proposed novel and simple approach to achieve large-angle scanning capability will also be explained. The scanning capability of linear arrays will be analyzed in Section III. The scanning performance of a planar array will be investigated in Section IV. Finally, the conclusion of this paper will be given.

II. The Design Principle And Methodology Analysis

A. *Antenna element geometry and design*

Fig. 1 (a) shows the three-dimensional view of the element which has a compact structure. It mainly consists of three parts: a radiating patch on a thin substrate (with a relative dielectric constant of 3.55, and the thickness of 1.524mm), a substrate with air-cavity (which is the poly-tetra propylene with a relative dielectric constant of 2.2), and a ground plane. The proposed element is excited by the coaxial probe. The key design parameters and stack diagram of the proposed antenna element are given in Fig. 1 (a) and (c). The key parameters of the structure, optimized by simulation, are reported in Table I.

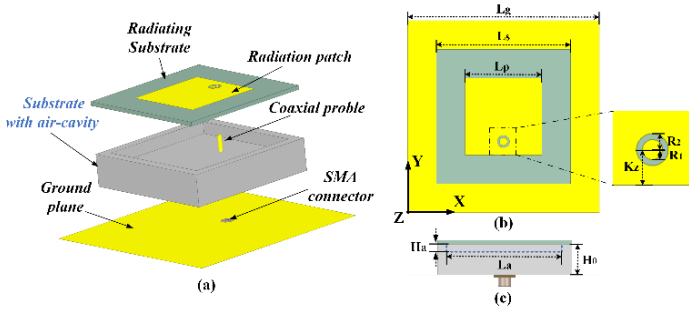

Fig. 1. The proposed antenna element: (a)3D view; (b)plan view; (c) side view.

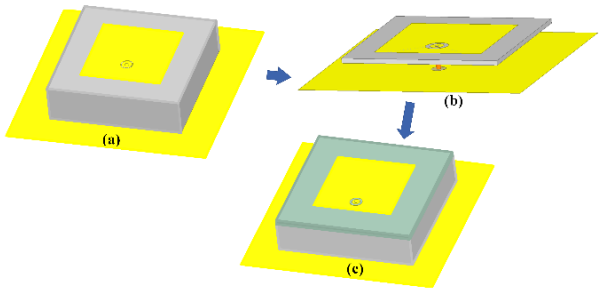

Fig. 2. Antenna design process: (a) Ant.1, (b) Ant. 2, (c) the proposed antenna.

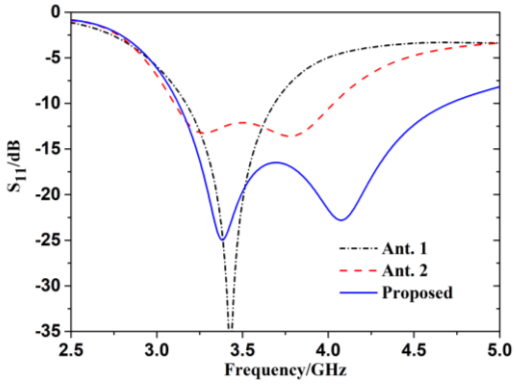

Fig. 3. Simulated reflection coefficients of three types of antennas.

As two key factors for designing phased arrays with the large-angle scanning capability, the inter-distance of elements in the array should enough small, and the antenna element should radiate wide beam in the array. Therefore, Fig.2 explains how to realize a patch antenna with a compact structure and wideband. Figure 3 shows the simulated return loss of three antennas. From Fig. 2 and Fig. 3, Ant. 1 is a general patch antenna (with a homogeneous and solid substrate) that exhibits a narrow bandwidth. To extend the work band of the antenna, an air layer is added to the structure. The bandwidth is broadened but the size is extended. Hence, a substrate with an air cavity and a Rogers RO4003C substrate are applied to expound the above-mentioned problem, as given in Fig. 2(c). The work band reported in Fig. 3, is from 3.1 GHz to 4.7 GHz (about 41%). The proposed antenna not only broadens the bandwidth and reduces the antenna size, but also improves the WAIM which will be explained in the following part.

TABLE I
DETAILED PARAMETERS OF THE ELEMENT

Parameter	Lg	Ls	Lp	R_1	R_2	Kz	La	H_0	Ha
Units (mm)	50	35	20	0.9	1.5	3.5	30	9	2

B. *The methodology analysis of this work*

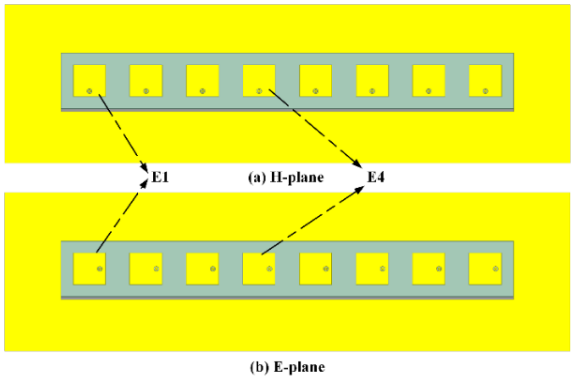

Fig. 4. Geometry of the linear array antennas.

Based on the proposed antenna element, linear array antennas in the H-plane and E-plane will be designed and analyzed in this section. Fig. 4 describes two linear arrays with eight cavity-substrate antenna elements, respectively. The size of rectangle ground is 350 × 100 mm^2, which is large enough to reduce the influence of the ground size on the beam scanning capability.

And it is conducive to studying the planar array scanning performance later. The distance adjacent elements in the array (*d*) is 35 mm.

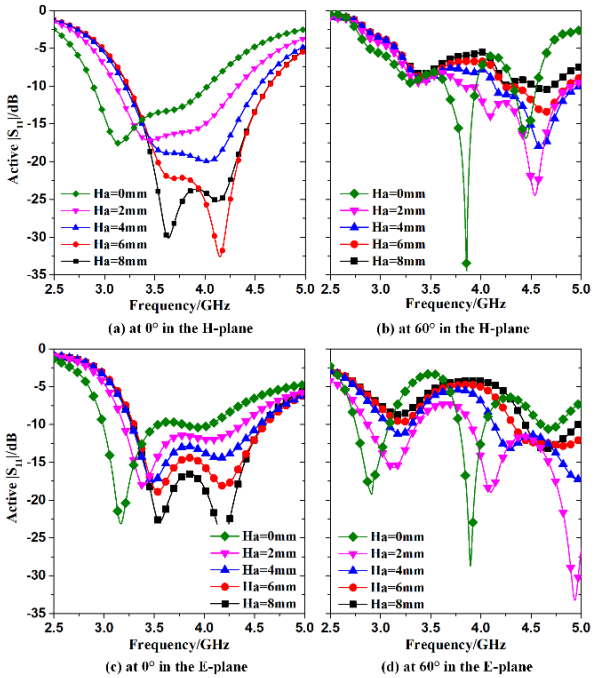

Fig. 5. Simulated active|S_{11}| of the center element in the H- and E-plane arrays with the variation of H_a.

As described earlier, the proposed structure with air-cavity substrates can improve the operating bandwidth as well as improving the impedance matching of the array elements at large coverage. As shown in Fig. 5, the active S-parameters with different air-cavity height (*Ha*) are given. We select the center element (E4) in the H- and E-plane linear arrays to explain the influence. For the H-plane array, the active |S_{11}| becomes worse and worse as the height of the air-cavity decreases, and the operating frequency band moves to lower frequencies when the antenna beam directs at broadside direction. Conversely, when the main beam directs at 60 degrees, the active |S_{11}| first improves and then worsens with the variation of the height. For the E-plane array, the tendency is similar to those of the H-plane array at broadside direction and 60 degrees with different the air-cavity height. We can find that the air cavity plays a pivotal role in improving the wide-angle scanning impedance though it is not the best for the impedance at broadside direction. Therefore, the air cavity height is an important parameter for the proposed array with large beam-scanning coverage. In addition, the air-cavity edge length (*La*) will also impact the array scanning performance. However, it is found that if *La* is large than *Lp*, the influence of *La* is very limited and can be negligible.

Moreover, the E-field distributions in two linear arrays are given to explain the effect on the radiating mechanism by the proposed approach, as shown in Fig. 6 and Fig. 7. By comparing the two types of E-field distributions, it is observed that the E-field distributions of two array antennas are very regular and similar when the main beams are at broadside direction. Eight antenna elements uniformly produce fundamental mode. Therefore, the sum of the E-field vector in the array is up to the strongest. However, when the beam of the array directs to a large angle, the E-field distribution of the array with Ant. 1 causes active impedance mismatch of the respective antenna element, so that the operating mode of some elements is different, and even some other operating modes are produced, as shown in Fig. 6(c). Hence, the sum of the electric field vector in the array leads to weakening. Oppositely, the sum of the electric vector in the array is up to the strongest whatever the beam scans at 0 or 60 degrees because of the substrate with the air-cavity improving WAIM of the array. The operating mode of every element in the array is the same as reported in Fig. 6(d).

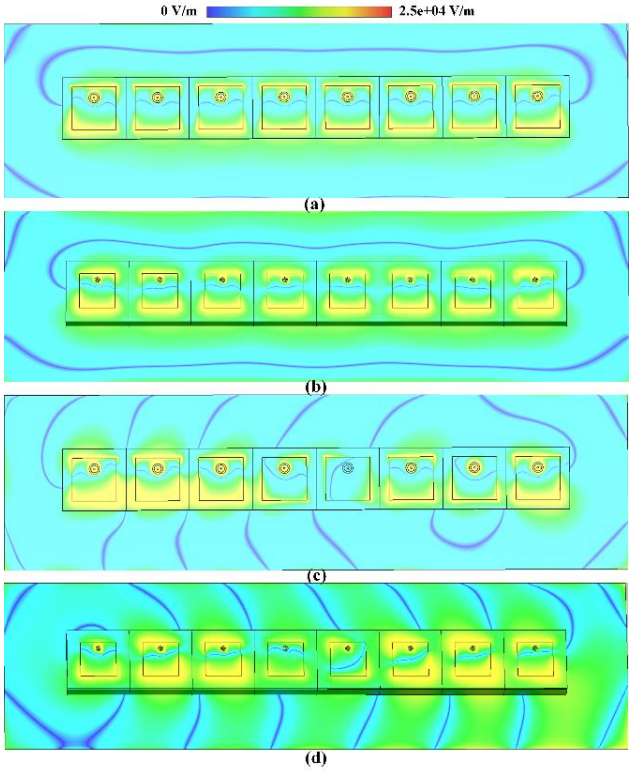

Fig. 6. E-field distribution of the H-plane array with Ant. 1 and the proposed antenna as array elements: (a) and (c) are Ant. 1 at 0° and 60°, respectively; (b) and (d) are the proposed antenna at 0° and 60°, respectively.

Similarly, the E-field distribution in the E-plane array is reported in Fig. 7. The proposed approach has also an effect on WAIM when the beam scans to the large coverage. The operating mode of every element in the array is the same, and the sum of the E-field vector is up to the strongest, as reported in Fig. 7(d). Therefore, this approach's mechanism for wide-angle impedance improvement is validated in both arrays, thereby achieving a large-angle scanning capability in the wide-bandwidth linear array.

The active wide-angle scanning impedance has been improved by the proposed approach. Another key factor is the proposed approach can make every element in the array produce a wide radiation pattern. It is a demonstration that the array radiation patterns are determined by the production of array factor and the array element radiation patterns [25]. Therefore, to realize large-angle scanning capability, not only the active impedance performance of the array must be enhanced, but also every element's pattern in the array should be broad. The simulated and measured radiation patterns of the antenna elements in two linear arrays are shown in Fig. 8. In the H-plane linear array, simulation

and experiment have good consistency. And they are wide-beam radiation patterns. It is the same as the E-plane array. The simulated results, in general, align with the measured results but there is a different shake curve in the E4, since the coupling in the array has an effect on it. However, it is also a wide-beam radiation pattern.

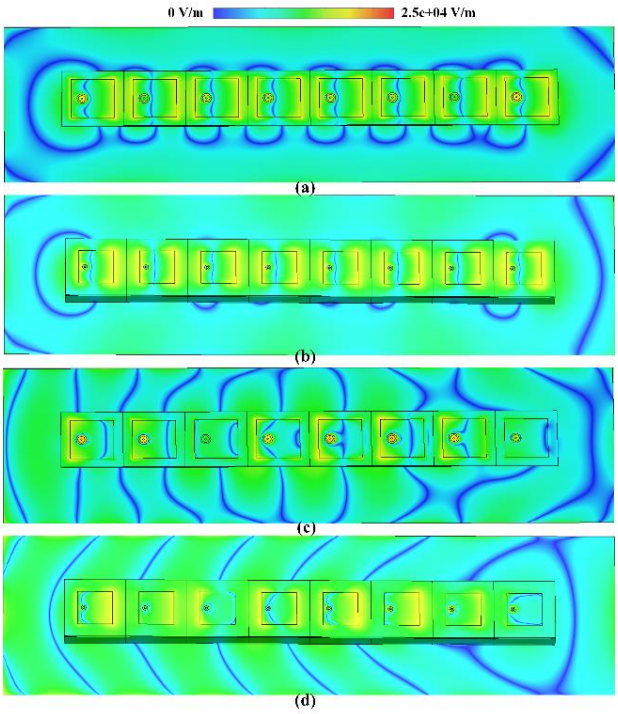

Fig. 7. E-field distribution of the E-plane arrays with Ant. 1 and the proposed antenna as array elements: (a) and (c) are Ant. 1 at 0° and 60°, respectively; (b) and (d) are the proposed antenna at 0° and 60°, respectively.

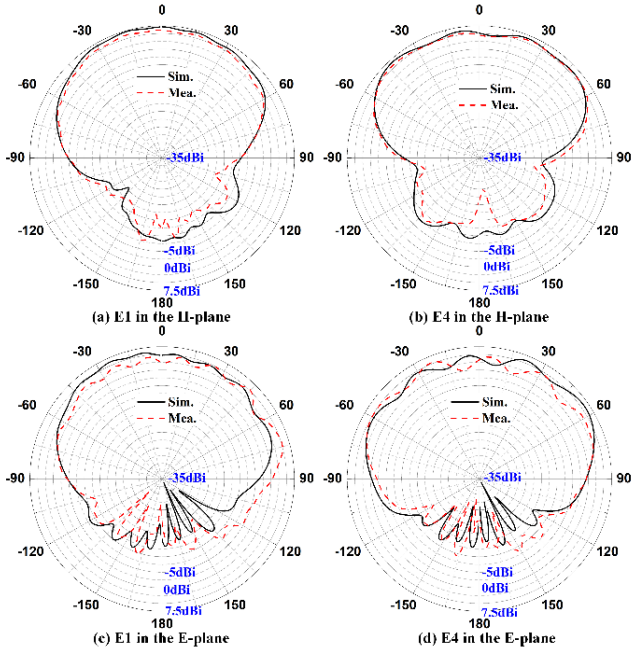

Fig. 8. Radiation patterns of the proposed antenna in the H- and E-plane linear arrays at 3.8 GHz.

To highlight the proposed simple and effective measures to enhance the wide-angle scanning coverage, Ant. 1 and Ant. 2 (see Fig. 2) are used to form linear array antennas which are similar to the proposed array antenna. The three arrays have the same ground size, element number, and inter-element spacing. The gain of three array antennas with varying scanning angles is shown in Fig. 9. We can clearly see that the scanning coverage with high gain of the proposed array antenna is much larger than that of the other two arrays in both H- and E-plane linear arrays within their respective operating bands. The beam of the array could scan to ±60° and ±70° with a realized gain reduction under 3dB in the wide bandwidth in the H-plane linear array and in the E-plane linear array, respectively. The realized gain of the proposed array at different frequencies and scanning angles is reported in Fig. 10. In the H-plane linear array as shown in Fig. 10(a), the realized gain first increases and then decreases with the scan angle increasing, and especially decreases steeply when the beam scans to more than 50° in the high-frequency band. In the H-plane linear array as given in Fig. 10(b), the change of the realized gain with varying scanning angles is relatively small, which is mainly due to the wider radiation patterns. But the gain has some fluctuations in the scanning coverage, which is mainly because of the mutual coupling in the array. We can also see these fluctuations from the element pattern in the array in Fig. 8.

Therefore, the proposed approach can improve the WAIM and give the broad beam-width of the array elements, simultaneously. Besides, the proposed approach can also be applied and realize the large-angle scanning characteristics through the verification of two linear arrays, which will further be explained in Section IV.

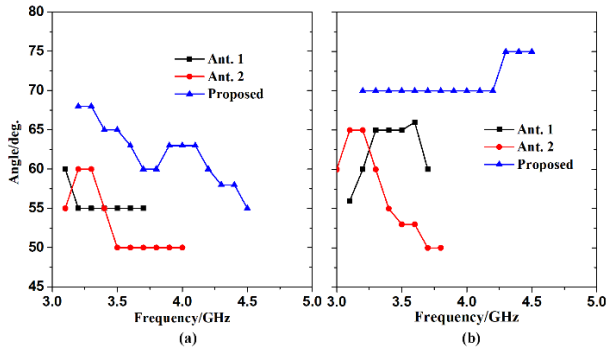

Fig. 9. Wide-angle scanning capability of three type array antennas with a gain reduction under less than 3dB in their respective bandwidths: (a) H-plane linear array and (b) E-plane linear array.

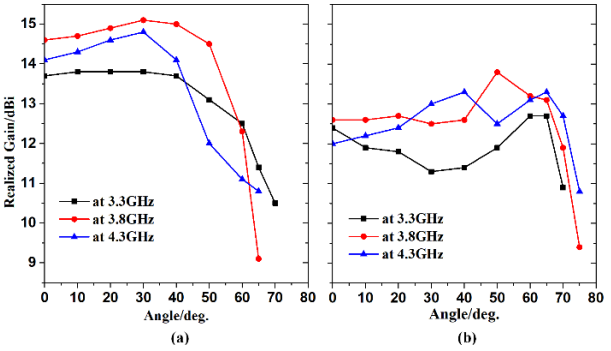

Fig. 10. Realized gain with varying scanning angles in different operating frequencies in (a) H-plane linear array and (b) E-plane linear array.

III. Scanning Capability Of The Array Antennas

A. The H-plane linear array

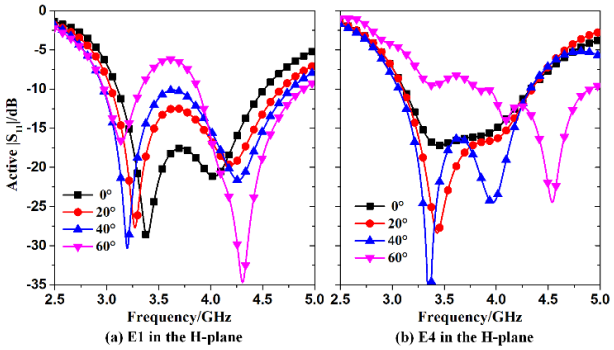

Fig. 11. Simulated active $|S_{11}|$ of the elements at different beam directions.

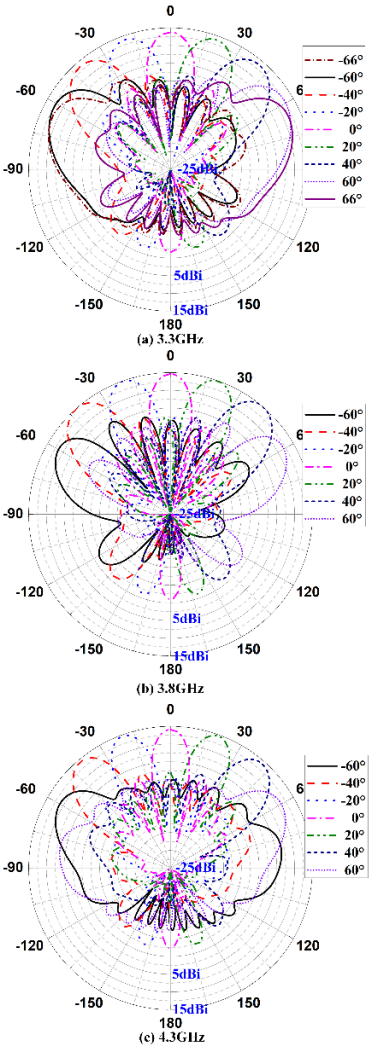

Fig. 12. Simulated scanning radiation patterns of the H-plane linear array antenna in the bandwidth.

The 1 × 8 H-plane linear array is presented and analyzed in Fig. 4 (a). The simulated active $|S_{11}|$ of elements in the array at different scanning angles are reported in Fig. 11. It is observed that the active $|S_{11}|$ is better than -10 dB within the frequency band when the beam directs at the scanning coverage of ±40°, while it is lower than -6dB when the beam scans up to 60°. Although there is some different variation of the active $|S_{11}|$ between E1 and E4, the active $|S_{11}|$ of all the antenna elements is still better than -6dB in the work band. Besides, the mutual coupling between the adjacent elements is less than -13 dB, while the mutual coupling in the array with Ant. 1 is just less than -10.5 dB. Therefore, the WAIM is mainly improved by the proposed approach, also gives slight enhancement of isolation. The simulated steering beams in the H-plane array are reported in Fig. 12. We still select the low (3.3 GHz), middle (3.8 GHz) and high (4.3 GHz) frequencies to elaborate the scanning characteristics of this array. We can find that when the scanning angle is less than 40 degrees, the realized gain of the array is almost the same, and the variation with scanning angles is relatively small. When the scanning angle is more than 50°, the gain drops a little faster. In addition, the best and worst sidelobes of the scanning beam are -13.5dB and -4.9dB in all the band, respectively. The detailed realized gain with the variation of scanning angles is shown in Fig. 10 (a).

B. The E-plane linear array

The simulated active $|S_{11}|$ of the elements in the E-plane linear array (see Fig. 4 (b)) at different scanning angles are given in Fig. 13. It is observed that the active $|S_{11}|$ is better than -10dB within the bandwidth when scanning coverage of the array is from 0° to 20°, and it is lower than -6dB when scanning from 0° to 70°. The mutual coupling in this array is similar to the one in the H-plane array. It is less than -12.5 dB, while the array with Ant.1 is better than -10.8 dB. The simulated radiation patterns in the array at 3.3 GHz, 3.8 GHz, and 4.3 GHz are reported in Fig. 14. It is observed that the realized gain in the low-frequency band firstly decreases and then increases with the scanning angles increasing, and the peak gain is at about 60°. The realized gain in the middle-frequency band is similar to the one in the low-frequency band. The realized gain in the high-frequency band firstly decreases and then increases with the scanning angles increasing from 0° to 65°. The detailed realized gain at different scanning angles and frequencies is given in Fig. 10 (b). The sidelobe of the beam directing to different angles in the whole frequency band is better than -10dB when the scanning angle is up to 60°. However, the worst sidelobe is -7.0dB in all the working band.

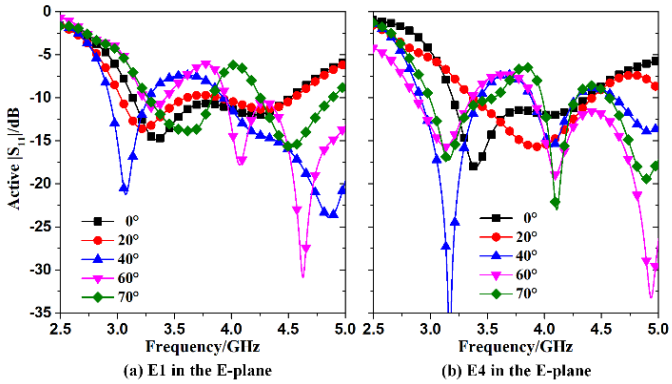

Fig. 13. Simulated active $|S_{11}|$ of the elements at different beam directions.

C. The measurement

The array design based on the proposed approach is validated by fabricating two 1 × 8 linear array antennas, depicted in Fig. 15. The antennas are fabricated according to the previous design requirements. Eight phased shifts and one 1-to-8 power driver are used to excite each element by providing the same amplitude and different phases, as given in Fig. 15(c). A SATIMO near-field measurement system is employed to text

the radiation patterns of the array as shown in Fig. 15(d). We still choose two typical antenna elements (one in the center and one at the end of the array) for measurement and verification. The measured return loss of two arrays (H-plane and E-plane arrays) are given in Fig. 16. From the figure, the measured results are very similar to the simulated results, especially in the H-plane linear array. For H-plane linear array, the impedance bandwidth (≤-10dB) is a wide frequency band (37.4%) and from 3.15 to 4.6 GHz. For the E-plane linear array, the impedance bandwidth (≤-10dB) is also a wide frequency band (39.0%) and from 3.1 to 4.6 GHz. Hence, we select three frequencies of the operating band to analyze the detailed scanning capability of the array. Also, the simulated and measured mutual coupling between the adjacent elements in the two arrays also is shown in Fig. 16. The measurements are very similar to the simulations. The mutual coupling is lower than -13 dB and -12.5 dB in the H- and E-plane arrays in the proposed work band, respectively. The proposed mutual coupling is a little high in the low-frequency band because of the closed inter-distance between elements which is about $0.37\lambda_l$ at 3.2 GHz.

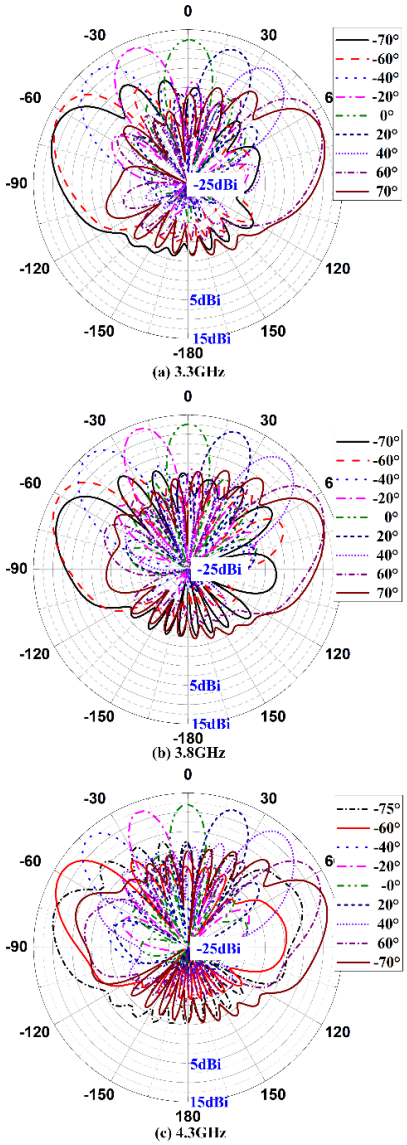

Fig. 14. Simulated scanning radiation patterns of the E-plane linear array antenna in the bandwidth.

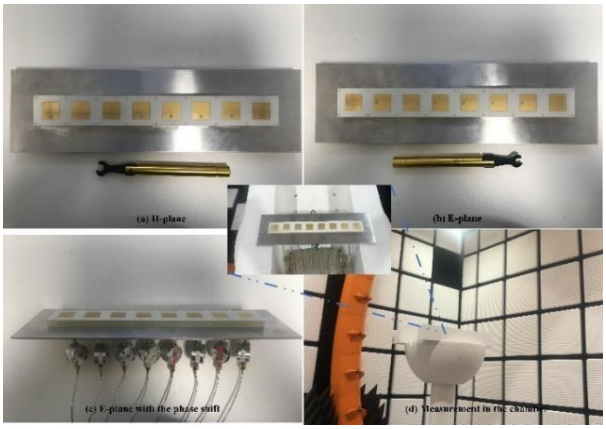

Fig. 15. Prototype of two arrays and detailed illustration for measurement.

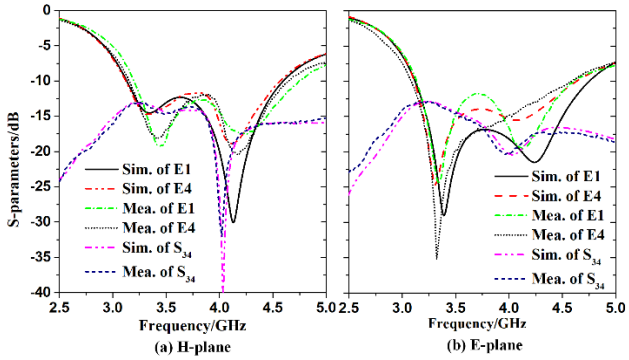

Fig. 16. Simulated and measured reflection coefficients of the proposed array antennas.

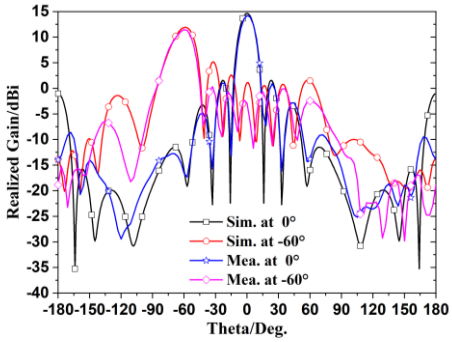

Fig. 17. Simulated and measured scanning radiation patterns of the H-plane linear array antenna at 3.8GHz.

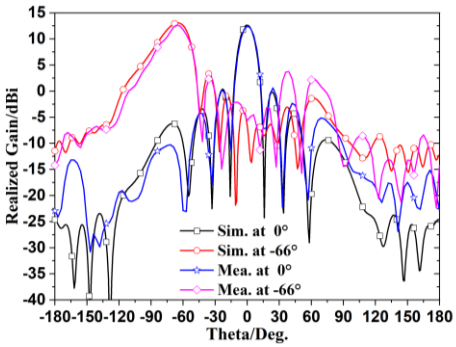

Fig. 18. Simulated and measured scanning radiation patterns of the E-plane linear array antenna at 3.8GHz.

To clearly analyze the simulated and measured results and demonstrate the arrays' scanning characteristics, the detailed comparison is shown in Fig. 17. The measurements align very well with the simulations, especially for the main-lobe,

regardless of the scanning beam at any direction. Similarly, the radiation patterns of the E-plane linear array, which are scanned to the broadside and -66°, are depicted in Fig. 18. Indeed, we can observe that the simulated and measured patterns are very similar. However, there is a little difference between the simulated and measured sidelobe. This is because each excited port has a little different amplitude, and the test scenario would affect the measured results. The measured radiation patterns of the H-plane array with the variation of scanning angles are shown in Fig. 19 (a-c). At 3.3GHz, the measured realized gain varies from 11 to 13.3dBi at the scanning coverage of ±66°, and the gain reduces less than 3dB. The sidelobes of the radiation beam become smaller as the scan angle increases. At 3.8GHz, the measured realized gain varies from 11.9 to 14.65dBi at the scanning coverage of ±66°, and the gain reduction is less than 3dB. At 4.3GHz, the measured realized gain varies from 11.5 to 14.2dBi at beam direction variation from -58° to 58°, and the gain reduction is less than 3dB. Additionally, the measured cross-polarized component remains 20 dB below the co-polarized component when the array scans to any directions. The radiation patterns at the other frequencies show similar agreement and were omitted for brevity. The best sidelobe of the scanning beam is -15.5dB and the worst sidelobe is -7.3dB in all the bandwidth.

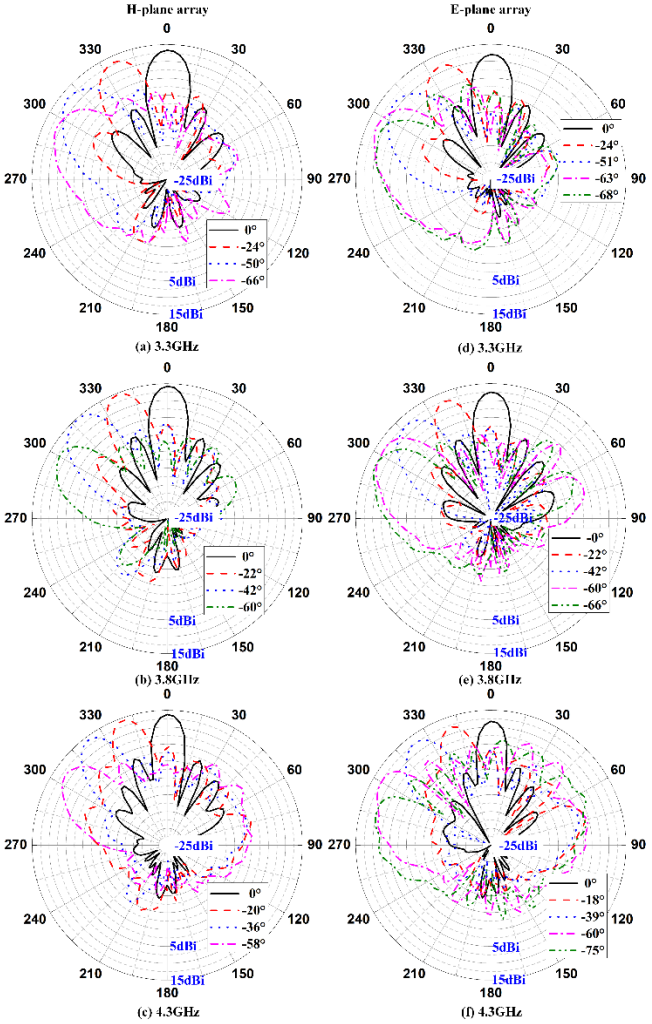

Fig. 19. Measured scanning patterns of the two arrays

The measured scanning patterns of the E-plane array are depicted in Fig. 19 (d-f). At 3.3GHz, the measured realized gain varies from 10.6 to 12.3dBi at the scan angle from -70° to 70°, and the gain fluctuation is less than 2dB. At 3.8GHz, the measured realized gain varies from 12.2 to 12.7dBi at the scan angle from -70° to 70°, and the gain fluctuation is less than 1dB. At 4.3GHz, the measured realized gain varies from 10.2 to 12.8dBi at the scan angle from -75° to 75°, and the gain fluctuation is less than 3dB. Additionally, the measured cross-polarized situation is similar to one of the H-plane array. The radiation patterns at the other frequencies also show similar agreement and were omitted for brevity. The best sidelobe of the scanning beam is -13.0dB and the worst sidelobe is -4.8dB in the whole frequency band. However, for the most scanning patterns in the whole frequency band, the sidelobe is less than -10dB, except for some high frequencies (over 4.2GHz). Therefore, the proposed linear array can realize the gain reduction under 3dB in the scanning coverage of ±70° in proposed operating band.

The excellent wide-angle scanning capability has been verified in the H- and E-plane linear array antennas in a wide frequency band with the proposed approach. It improves the WAIM and also achieves broad beam-width of the array elements. Hence, it is very promising to enhance large-angle scanning capability of the planar array with this approach.

IV. Wide-Angle Scanning Planar Phased Array

To demonstrate the effect of the proposed approach for the planar array, an 8 × 8 planar phased array is designed as given in Fig. 20. The proposed planar array layout is completely in line with the requirements of the linear array in the above sections: the same antenna element, the same element spacing, and the same structure. Therefore, the conclusion from the linear array would be verified in the planar array of this section.

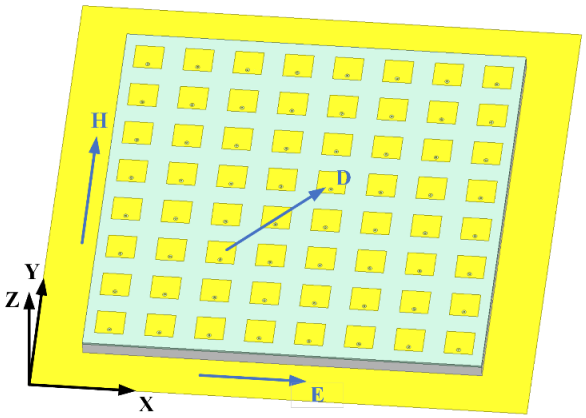

Fig. 20. The configuration of the planar array antenna.

In Fig. 21, the planar array using the same elements and requirements is presented. To evaluate the overall array scanning performance, the realized gain at different scanning angles in the operating frequency band is given and studied in this section. In the H-plane (*yoz*-plane), we can see that the realized gain drops slowly when the beam scans from 0° to 40°, but declines more when scanning to 40°, as given in Fig. 21(a). The simulated scanning patterns in the H-plane at three different frequencies (3.3 GHz, 3.8 GHz, 4.3 GHz) are presented in Fig. 21 (b-d). It is

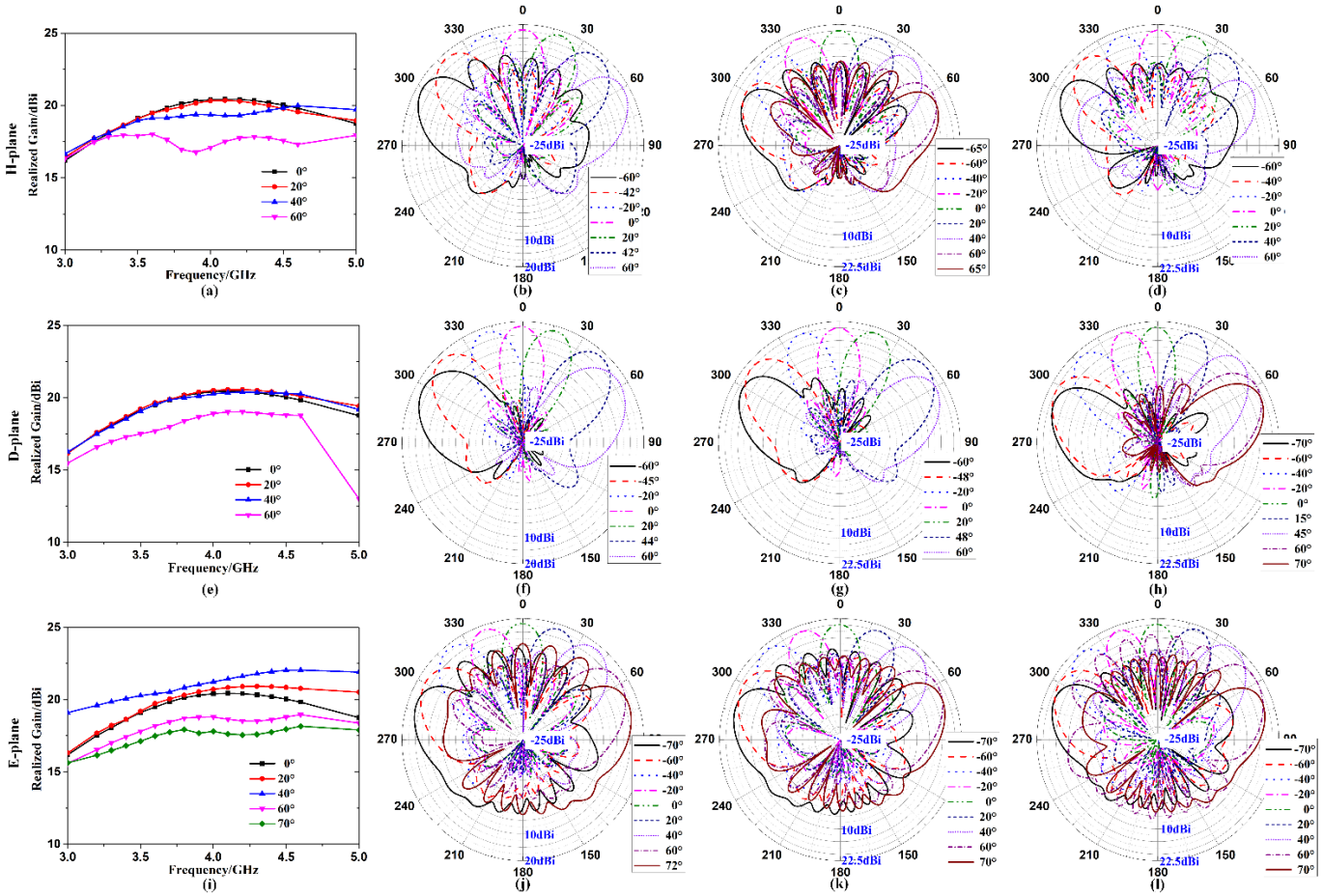

Fig. 21. Wide-angle scanning performance of the planar array antenna.

observed that the realized gain in the low-frequency band barely changes with the scanning angles increasing. However, the realized gain in the middle-part of the operating band drops more with larger scanning angles but the variation is less than 3dB. And the realized gain in the high-frequency band drops less than 3.5 dB. The array sidelobes increase with larger scanning angles. The worst sidelobe level is -4.8dB, where the beam is at high-frequency at 60°. In the D-plane (diagonal plane), we can find that the realized gain hardly changes with the increase of the scanning angle, and only drop a little when the beam scans to 60°, as given in Fig. 21(e). In the D-plane, the scanning beam at three typical frequencies (3.3 GHz, 3.8 GHz, 4.3 GHz) are given in Fig. 21 (f-h). The scanning coverage of the beam is ±60° with a realized gain reduction under 3dB. The sidelobe level in D-plane is very low and below -20dB in the whole band. In the E-plane (*xoz*-plane), the scanning coverage with a realized gain reduction under 3dB is significantly larger than that of the other two planes, and is consistent with the conclusion obtained by the E-plane linear array. As depicted in Fig. 21(i), the realized gain increases firstly when the beam scans from 0° to 40°, then decreases when the beam scans from 40° to 70°. The above phenomenon is similar to the one in the E-plane linear array, which can confirm that the feasibility of the planar array characteristics can be deduced from the linear array characteristics. The simulated scanning beam at three typical frequencies (3.3 GHz, 3.8 GHz, 4.3 GHz) in the E-plane are presented in Fig. 21 (j-l). The scanning coverage of the beam is ±70° with a realized gain reduction under 3dB. The sidelobe of the scanning beam in the whole band is less than -10dB when the scanning coverage is ±60°. From the above analysis, a wide band planar phased array is studied and realized to scan from -60° to +60° with a realized gain reduction under 3.5dB in two-dimensional space in the wide operating band. More specifically, the antenna in the E-plane can scan to ±70°.

V. Conclusion

The proposed work presents a wide-band phased array antenna with large scanning coverage for the mobile communication system. One simple and efficacious approach, which is mix-substrate with air-cavity is applied to enhance the scanning coverage and bandwidth of the phased array. Firstly, the wide-angle scanning impedance matching could be improved, especially the one at the large scanning angle, which is adjusted by the height of the air-cavity. Besides, the proposed approach is also good radiate wide patterns for every element in the array, which is a key factor to enhance scanning capability. Subsequently, the operating frequency band is extended by the proposed compact structure. By analysis of the active reflection coefficient at large scanning coverage and comparison with common patch antenna in the E-filed, and analysis of the radiation patterns of the elements in the array, the proposed approach is verified to enhance the scanning

capacity of the array in detail. Two 1×8 linear arrays and one 8×8 planar array are demonstrated, which achieve the large scanning coverage of around ±60° but a realized gain reduction under 3.5 dB in the band from 3.15 to 4.6 GHz (37.4%). Furthermore, the beam in the E-plane can scan more than ±70° with a realized gain reduction under 3 dB. Two linear array prototypes for wide-angle scanning capacity in the H- and E-plane are fabricated and characterized, yielding good performance with overall operational bandwidth. The wide band phased array with large scanning coverage can be realized by the proposed approach and applied in mobile communication system.

REFERENCES

[1] N. Amitay, V. Galindo, and C. P. Wu, Theory and Analysis of Phased Array Antennas. New York, NY, USA: Wiley-Interscience, 1972.

[2] J. Zhang, X. Ge, Q. Li, M. Guizani, and Y. Zhang, "5G millimeter-wave antenna array: Design and challenges," *IEEE Wireless Communications,* vol.24, no. 2, pp. 106-112, Apr. 2007.

[3] S. E. Valavan, D. Tran, A. G. Yarovoy, A. G. Roederer, "Planar Dual-Band Wide-Scan Phased Array in X-Band," *IEEE Transactions on Antennas & Propagation*, vol. 62, no. 10, pp. 5370-5375, Oct. 2014.

[4] R. Wang, B. Z. Wang, C. Hu, and X. Ding, "Wide-Angle Scanning Planar Array with Quasi-Hemispherical-Pattern Elements," *Scientific Reports*, vol. 7, no. 1, pp. 2729, Jun. 2017.

[5] G. Yang, J. Li, S. G. Zhou, Y. Qi. "A Wide-Angle Scanning E-plane Linear Array Antenna with Wide Beam Elements," *IEEE Antennas Wireless Propag. Lett.*, vol. 16, pp. 2923–2926, Oct. 2017.

[6] A. Kedar and K. S. Beenamole. "Wide Beam Tapered Slot Antenna for Wide-angle Scanning Phased Array Antenna," *Progress in Electromagnetics Research B*, vol. 08, no. 1, pp. 235-251, 2011.

[7] K. S. Beenamole, P. N. S. Kutiyal, U. K. Revankar, and V. M. Pandharipande, "Resonant Microstrip Meander Line Antenna Element for Wide Scan Angle Active Phased Array Antennas," *Microwave & Optical Technology Letters*, vol. 50, no. 7, pp. 1737-1740, 2010.

[8] G. Yang, J. Li, D. Wei, R. Xu, "Study on Wide-Angle Scanning Linear Phased Array Antenna," *IEEE Transactions on Antennas and Propagation*, vol. 66, no. 1, pp.450-455, Jan. 2018.

[9] Y. F. Cheng, X. Ding, W. Shao, & B. Z. Wang, "Planar wide-angle scanning phased array with pattern-reconfigurable windmill-shaped loop elements," *IEEE Transactions on Antennas and Propagation*, vol. 65, no. 2, pp. 932-936, Feb. 2017.

[10] H. Tian, L. J. Jiang, and T. Itoh, "A Compact Single-Element Pattern Reconfigurable Antenna with Wide-Angle Scanning Tuned by a Single Varactor," *Progress in Electromagnetics Research C*, Vol. 92, 137-150, 2019.

[11] Z. Jiang, S. Xiao, Y. Li, "A wide-angle time-domain electronically scanned array based on energy-pattern-reconfigurable elements," *IEEE Antennas and Wireless Propagation Letters*, vol. 17, pp. 1598-1602, Jul. 2018.

[12] E. G. Magil, H. A. Wheeler, "Wide-Angle Impedance Matching of A Planar Array Antenna by A Dielectric Sheet," *IEEE Transactions on Antennas and Propagation*, vol. 14, no. 1, pp. 49-53, 1966.

[13] P. Munk, "On Arrays that Maintain Superior CP and Constant Scan Impedance for Large Scan Angles," *IEEE Transactions on Antennas and Propagation*, vol. 51, no. 2, pp. 322-330, Apr. 2003.

[14] M. N. M. Kehn, L. Shafai, "Improved Matching of Waveguide Focal Plane Arrays Using Patch Array Covers as Compared to Conventional Dielectric Sheets," *IEEE Transactions on Antennas and Propagation*, vol. 57, no. 10, pp. 3062-3076, Jul. 2009.

[15] T. R. Cameron, and G. V. Eleftheriades, "Analysis and Characterization of a Wide-Angle Impedance Matching Metasurface for Dipole Phased Arrays," *IEEE Transactions on Antennas and Propagation*, vol. 63, no. 9, pp. 3928-3938, Sept. 2015.

[16] A. G. Toshev. "Multipanel Concept for Wide-Angle Scanning of Phased Array Antennas," *IEEE Transactions on Antennas and Propagation*, vol. 56, no. 10, pp. 3330-3337, Oct. 2008.

[17] N. H. Noordin, T. Arsian, B. Flynn, A. T. Erdogan, "Low-Cost Antenna Array with Wide Scan Angle Property," *IET Microwaves Antennas & Propagation*, vol. 6, no. 15, pp. 1717-1727, Dec. 2012.

[18] K. Liu, S. Yang, S. W. Qu, C. Chen, Y. Chen, "Phased hemispherical lens antenna for 1-D wide-angle beam scanning," *IEEE Transactions on Antennas and Propagation*, vol. 67, no. 12, pp. 7617-7621, Dec. 2019.

[19] D. K. Papantonis, J. L. Volaki, "Dual Polarized Tightly Coupled Array with Substrate Loading," IEEE Antennas and Wireless Propagation Letters, vol. 15, pp. 325-328, Jun. 2015.

[20] E. Yetisir, N. Ghalichechian, J.L. Volakis, "Ultrawideband Array with 70° Scanning Using FSS Superstrate," IEEE Transactions on Antennas and Propagation, vol. 64, no. 10, pp. 4256-4265, Jul. 2016.

[21] Y. Zhang, S. Zhang, J. Li and G. F. Pedersen, "A Transmission-Line-Based Decoupling Method for MIMO Antenna Arrays," IEEE Transactions on Antennas and Propagation, vol. 67, no. 5, pp. 3117-3131, May 2019.

[22] A. K. Singh, M. P. Abegaonkar and S. K. Koul, "Wide Angle Beam Steerable High Gain Flat Top Beam Antenna Using Graded Index Metasurface Lens," IEEE Transactions on Antennas and Propagation, vol. 67, no. 10, pp. 6334-6343, Oct. 2019.

[23] Y. Lv, X. Ding, B. Wang and D. E. Anagnostou, "Scanning Range Expansion of Planar Phased Arrays Using Metasurfaces," IEEE Transactions on Antennas and Propagation, vol. 68, no. 3, pp. 1402-1410, March 2020.

[24] H. Xu, S. Xu, F. Yang and M. Li, "Design and Experiment of a Dual-band 1-bit Reconfigurable Reflectarray Antenna with Independent Large-angle Beam Scanning Capability," IEEE Antennas and Wireless Propagation Letters, early access.

[25] C. C. Liu, J. Shmoys, and A. Hessel, "E-plane performance trade-offs in two-dimensional microstrip-patch element phased-arrays," *IEEE Trans. Antennas Propag.*, vol. 30, no. 6, pp. 1201–1206, Nov. 1982.

Guang-Wei Yang (S'15-M'19) received the B.E., M.S., and PhD. Degrees all in Electronic Engineering in Northwestern Polytechnial University in 2012, 2015, 2019, respectively. He is currently working at Queen Mary University of London as a Royal Society-Newton International Fellow. He was a Postdoc in the Antenna, Propagation and Millimeter-wave Systems (APMS) Section, Aalborg University, Denmark from 2019 to 2020. This author became a Student Member of IEEE in 2015. He also serves as a reviewer for all the IEEE and IET journals related to antennas. His recent research interests include microstrip antennas, wideband antennas, millimeter-wave array antennas, circularly-polarized antennas, base station antennas, phased array antennas, reconfigurable antennas, wide-angle scanning antenna and EM Periodic Structure

Yi-Ming Zhang (S'17) received the B.S. and M.S. degrees from Central China Normal University in 2008 and University of Electronic Science and Technology of China in 2014, respectively, and the PhD degree from University of Electronic Science and Technology of China in 2019. He is now working toward the Postdoc in the Antenna, Propagation and Millimeter-wave Systems (APMS) Section, Aalborg University, Denmark. Since February 2018, he has been a guest researcher with the Antenna, Propagation and Millimeter-wave Systems (APMS) Section, Aalborg University, Denmark. His current research interests include MIMO antenna decoupling, single-channel full-duplex communications, and passive RF and microwave components.

Shuai Zhang (SM'18) received the B.E. degree from the University of Electronic Science and Technology of China, Chengdu, China, in 2007 and the Ph.D. degree in electromagnetic engineering from the Royal Institute of Technology (KTH), Stockholm, Sweden, in 2013. After his Ph.D. studies, he was a Research Fellow at KTH. In April 2014, he joined Aalborg University, Denmark, where he currently works as Associate Professor. In 2010 and 2011, he was a Visiting Researcher at Lund University, Sweden and at Sony Mobile Communications AB, Sweden, respectively. He was also an external antenna specialist at Bang & Olufsen, Denmark from 2016-2017. He has coauthored over 80 articles in well-reputed international journals and over 16 (US or WO) patents. His current research interests include: mobile terminal mm-wave antennas, biological effects, CubeSat antennas, Massive MIMO antenna arrays, UWB wind turbine blade deflection sensing, and RFID antennas.